WATER-BASED RANKINE-CYCLE WASTE HEAT RECOVERY SYSTEMS FOR ENGINES: CHALLENGES AND OPPORTUNITIES

Gunnar Latz[1]*, Olof Erlandsson[2], Thomas Skåre[2], Arnaud Contet[2],
Sven Andersson[1] and Karin Munch[1]

[1]Chalmers University of Technology, Department of Applied Mechanics,
Gothenburg, Sweden
e-mail: latz@chalmers.se, sven.b.andersson@chalmers.se, karin.munch@chalmers.se

[2] TitanX Engine Cooling,
Sölvesborg, Sweden
e-mail: olof.erlandsson@titanx.com, thomas.skare@titanx.com, arnaud.contet@titanx.com

ABSTRACT

Much of the fuel energy in an internal combustion engine is lost as heat, mainly through hot exhaust gas. The high energy losses, and high temperatures of the exhaust gas, provide favorable conditions for applying a waste-heat recovery system. Among the available options, systems based on the Rankine cycle show the highest potential in terms of reducing fuel consumption.

Water or water-based mixtures have several advantages over organic fluids as working fluids for such applications of the Rankine cycle, in terms of cost, thermal stability, safety and complexity of the system. They also have several disadvantages, including possible freezing for pure water, high boiling temperature and high heat of vaporization. Hence, higher temperatures and amounts of waste heat are needed for reliable operation of the system. However, few experimental investigations have addressed the practical challenges associated with water and their effects on the performance and operation of a system in a driving cycle.

This paper presents results of experiments with a full-scale system for recovering waste heat from the exhaust gas recirculation (EGR) of a 12.8 L heavy-duty Diesel engine on a test bench. The working fluid used in the experiments was deionized water and a 2-cylinder piston expander served as an expansion device. The engine was kept in standard configuration, except for minor modifications required to implement the heat-recovery system. The prototype EGR boiler was designed to fit in the space initially designated for the production EGR cooler.

The assembly was operated in the operating points of the European Stationary Cycle (ESC). The results show that the trade-off between boiling pressure, sufficient superheating of the water and cooling of the EGR caused by the pinch-point in the boiler poses a major challenge when using water as a fluid. Low flow rates at low load points were challenging for boiler stability. During operation, the blow-by of working fluid into the lubrication system of the expander and vice versa was also problematic. Special steam-engine oil with high viscosity and good water separation capability was used to weaken this effect. The Rankine cycle-based test system attained a thermal efficiency of 10% with EGR as the only heat source. Results, major constraints and possible means to improve the system when using water as a working fluid are presented here. Simulation models developed for the EGR boiler and the piston expander supported this effort.

1. INTRODUCTION

Most of the fuel energy in an internal combustion engine is lost as heat. These losses can be reduced by using waste-heat recovery (WHR) systems, which have been widely discussed and investigated by various research groups in the last decade, as extensively reviewed by Sprouse and Depcik (2013) and Wang *et al*. (2011). Systems based on the Rankine cycle have been identified as the most appropriate for vehicle applications, in terms of efficiency, maturity and cost. Such systems could potentially increase the powertrain efficiency of long-haul trucks (for which operating conditions are considered particularly suitable) by up to 30%, according to Wang *et al.* (2011). The most commonly discussed heat sources of the combustion engine are (in increasing order of temperature and hence quality of the utilizable heat) the engine coolant, charge air cooler, tailpipe exhaust gas and exhaust gas recirculation (EGR) system. Horst *et al.* (2014) noted that both charge air cooler and EGR are particularly attractive for heat recovery applications, since the recovered energy is removed from the load on the vehicle cooling system, while utilizing tailpipe exhaust gas adds additional heat to it.

Besides the choice of the heat source, the two main components that affect the conceptual design and performance are the working fluid used in the cycle and the expansion device, which is used to expand the generated vapor and produce the output work of the cycle. Optimal choices of the components are interdependent and depend on both the boundary conditions and requirements of the heat-recovery system (Seher *et al.,* 2012; Latz *et al.,* 2013). There are two main categories, based on the selected working fluid: organic Rankine cycle (ORC) if organic fluids are used and the traditional steam Rankine cycle if water is used.

Panesar *et al.* (2013) compared organic working fluids for a Euro 6 heavy-duty Diesel engine concept with high EGR rate, and concluded that acetone, R30 and R1130 provided better performance (under the chosen boundary conditions) than water, which was included in the tests for comparison. The drawback of water was the large amount of heat required to evaporate and superheat it, which reduced overall conversion efficiency. However, the cited authors noted that water also had substantial advantages, including its high thermal conductivity and absence of any health, environmental and safety issues. These advantages were also highlighted by Stobart and Weerasinghe (2006), who decided that water would be the most practical fluid to use in vehicle applications if the freezing issue could be overcome. Furthermore, Rayegan and Tao (2009) summarized the literature and concluded that no available organic fluid has all the desirable characteristics for an ORC application. Accordingly, Struzyna *et al.* (2014) found that various organics, including ethanol, acetales, siloxanes and ethers, lack long-term thermal stability at 275°C (the most stable were alkanes, cycloalkanes, aromatics and fluorinated hydrocarbons).

Two general conclusions that can be drawn from previous studies are that as heat-source temperatures rise beyond ca. 300°C (Ringler *et al.*, 2009) or 370°C (Sprouse and Depcik, 2013) the most efficient option switches from ORC to the steam Rankine cycle, and that neither option is clearly superior for applications at typical heavy-duty exhaust temperatures. However, at most operating points, temperatures in the high-pressure EGR system are higher than the 300-370°C threshold, and thus more suitable for steam systems, both theoretically and in terms of thermal stability of the fluid. Thus, several research groups have considered the performance of a heat-recovery system using EGR as a heat source and pure water or water-based mixtures as a working fluid (Howell *et al.*, 2011; Edwards *et al.*, 2012; Seher et al., 2012). However, these studies have paid little attention to the operational challenges raised by using water as a fluid in a full-scale test system, such as the major limitations when using water as a fluid, interactions between the EGR and heat-recovery system, and key aspects of the expander design. Hence, the focal concerns of the study presented here were the operational challenges and bottlenecks related to the components of such systems, rather than the system performance *per se*.

2. METHODOLOGY

This section briefly describes the experimental setup, the tests performed and simulations undertaken to support the experiments.

2.1 Experimental setup and components

The WHR system examined in this study utilized heat from the high-pressure EGR route of a heavy-duty Diesel engine. **Figure 1** displays the system layout and details of the measurement equipment used to obtain the presented results. The water used as working fluid in the system was deionized, to avoid scale forming in the boiler. An observation glass was installed between the boiler and expander in order to check whether the working fluid was fully superheated or still in a two-phase state. The system was developed as a flexible tool for research purposes, neglecting packaging issues related to vehicle design, except that the EGR boiler replaced the production EGR cooler with only minor modifications to the bracketing on the engine.

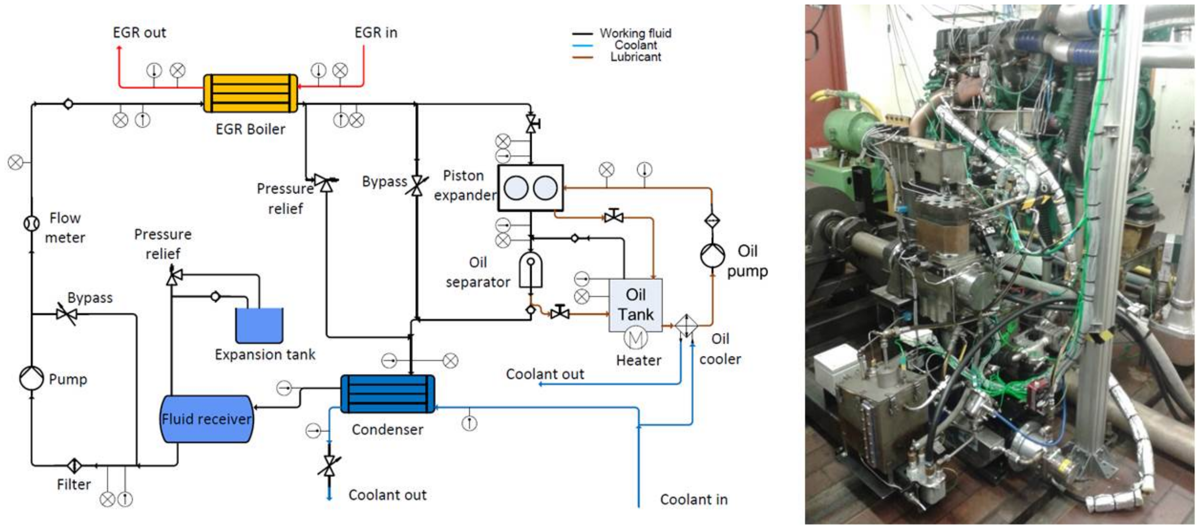

Variable	Sensor principle	Range	Accuracy
Flow-rate (working fluid)	Coriolis	0 – 2.72 kg/h	0.2% of reading
Flow-rate (EGR)	Venturi with Δp-sensor	0-350 mbar	2% of reading (Δp)
Flow-rate (coolant)	Turbine flowmeter	0.8 – 80 liter/minute	2% of reading
Temperature	Thermocouple (K-type)	-40°C – 1100°C	< 2.4°C @ max. 600°C
Pressure	Piezoresistive	0 – 10 bar and 0 – 60 bar	0.25% of range

Figure 1: Experimental system layout and specification of the measurement equipment

The expansion device used in the heat-recovery system was a 2-cylinder, uni-flow (Stumpf, 1912) piston expander, in which live steam enters at the top of the cylinder and leaves after expansion through exhaust ports in the cylinder wall near the bottom dead center position of the piston (**Figure 2**). The inlet valve of the piston expander is actuated from inside the cylinder by a push-rod, driven by an eccentric cam sitting on top of the con-rod. The steam gets highly re-compressed after the piston closes the exhaust port on its way to top dead center. This reduces losses at the steam inlet, but sufficiently high live steam pressure and sufficiently low exhaust steam pressure are needed for the expander to produce any power. Tests with the presented expander showed that its operation required the live steam pressure to be at least 17 bar if the steam outlet pressure was 1 bar. Initially, it was designed for running on ethanol in a system utilizing more than only EGR heat, thus it was not expected to be optimal for the setup applied here (where 30 bar was the maximum specified pressure for the EGR boiler). However, the effect of this design drawback was one of the phenomena examined in the study.

A counter-flow plate heat-exchanger was constructed using plate-and-bar technology to operate as an EGR-boiler (evaporator), **Figure 2**. The height and length were set by the space available when it replaced the engine's original EGR cooler, but the width was allowed to increase. Vertical plates were used to investigate the effects of gravity and phase separation.

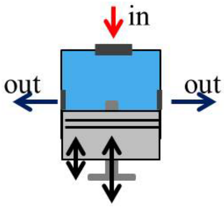

Bore/ stroke	90 mm/60 mm
Valve timing	Inlet opening: 17° before TDC Inlet closing: 34° after TDC Exhaust opening/closing: 110° after TDC/before TDC
Compression ratio	21 (geometric)

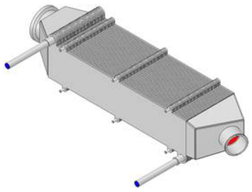

Channels	Fluid: 22 Gas: 21
Fin geometry	Offset strip fin (OSF), strips along the flow
Core size (effective)	Length: 458 mm Height: 95 mm

Figure 2: Schematic diagram and geometry of the uni-flow expander (upper image and table) and the EGR boiler (lower image and table)

Since this heat exchanger was considered to be a functional prototype for limited testing, no special measures were taken to minimize corrosion. The plates and turbulators were made of stainless steel and it was copper-brazed (vacuum), which was deemed acceptable for purposes of this study.

2.2 Experiments

To evaluate the potential for recovering heat from the EGR, the experimental system was operated with the expander bypassed to avoid oil contamination from its lubrication system. This would otherwise have affected the performance and reproducibility of the boiler tests. In these experiments the expander-bypass valve controlled the boiling pressure. However, tests with the expander engaged were also performed to validate the potential power output with the current expander design and the severity of the oil contamination issue.

2.3 Piston expander and EGR boiler simulations

A detailed model of the piston expander was implemented in the commercial 1-D flow simulation package GT-Suite. The model was then utilized to investigate optimal parameters for the expander and its performance limits when using water as a fluid in the heat-recovery system.

The boiler was sized using a TitanX in-house design tool based on a 0D lumped-element model (LEM) in Matlab®. The modeled heat exchanger was discretized into 20 elements along the flows (**Figure 3**) and all the channels were assumed to be under the same conditions. Partial boiling was allowed in elements, and where this occurred the overall heat transfer was iteratively weighted from boiling and single phase enthalpy parts to match the boiling start/end heat transfer energies. Cross-flow at entry and exits on the fluid side turbulator were ignored in the simulations. Factors and assumptions used are listed in **Table 1**.

Table 1: Factors and assumptions used for the boiler model

Modelling issue	Correlations/assumptions	Reference(s)
OSF heat transfer and pressure drop	Manglik/Bergles (single phase), Mandrusik/Carey (vaporization), Cooper (nucleate boiling for plain surface component)	Webb and Kim (2005)
Fluid properties	NIST Refprop data for water	Lemmon *et al.* (2013), Wagner and Pruss (2002)
Pressure drops	Single pressure drop factors (factors on dynamic pressure, evaluated at local conditions) • 1.4 at boiler connections (at restriction flow area) • 1.0 at inlet/outlet to channels (on turbulator flow area)	-

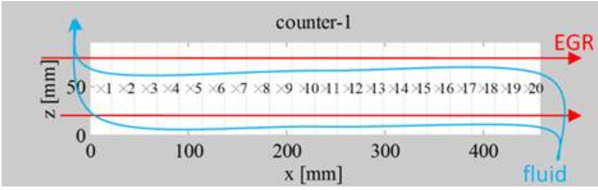

Figure 3: Discretization of the boiler in the lumped-element model.

In addition to the LEM, a working CFD model was developed at TitanX, with overall goals to investigate qualitatively and characterize local flow phenomena in fluid channels (and to a lesser extent) predict overall heat-exchanger performance. This CFD model, established in ANSYS Fluent, describes a single fluid and a single gas channel, as two separate CFD domains. The local projected heat transfer between the two domains is modeled from the LEM simulation described above and implemented as a continuous user-defined function (UDF). Variations in heat transfer strongly depend on the phase on the fluid side, thus the model uses fluid enthalpy as a parameter for the projected heat transfer coefficient (**Figure 4**). It should be noted that the model is only valid for one particular pressure, to characterize the specified heat transfer configuration, so it only provides qualitative results. The CFD model uses porous media for describing the offset strip fin (OSF) resistance, with differences in resistance along and across the fins (in a separate detailed module). It extends the analytic abilities provided by the LEM, by allowing exploration of effects on the system of fluid separation, inertia, gravity and variations of flows in the channels.

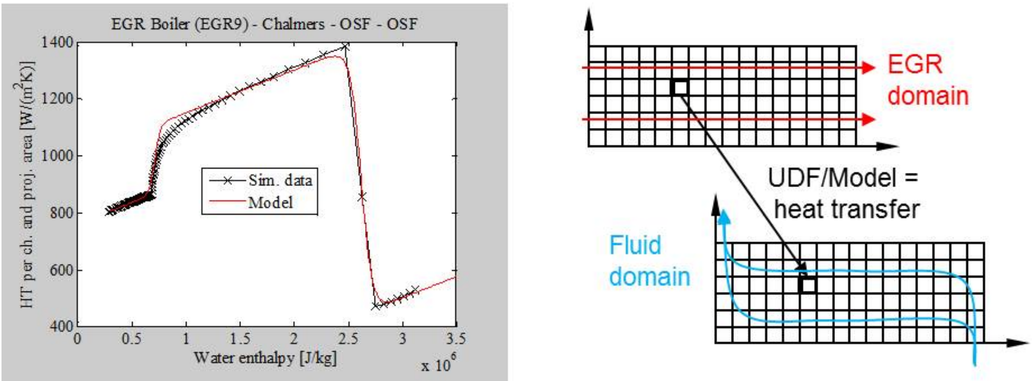

Figure 4: UDF ("Model") describing projected heat transfer per channel and projected plate area. The principle of the UDF is illustrated by the figure to the right, showing CFD representations of an EGR- and a fluid channel.

3. RESULTS

This section presents findings from experiments with the system described above and complementary simulations of the piston expander and EGR boiler.

3.1 Experiments with the bypassed system at ESC points

The performance of the heat recovery system, in terms of heat transfer from the EGR, and EGR cooling capability, is displayed in **Figure 5**. Superheating clearly occurred at all covered ESC points and considered boiling pressures. The 25% load cases are excluded since it was not possible to achieve stable superheating at these points due to low EGR temperatures and flow. The engine could not be operated at full load with the applied setup either, due to limitations of the dynamometer. A problem associated with water, compared to organic fluids, is its limited capability to cool the EGR, mainly due to the high boiling temperatures and heat of evaporation, as previously reported in the theoretical study by Panesar *et al.* (2013). Hence, during the experiments reported here the EGR temperatures at the higher load points and boiling pressures were around 200ºC, more than double the temperatures (in degrees Celsius) maintained with the production EGR cooler, requiring corrective actions to the setup.

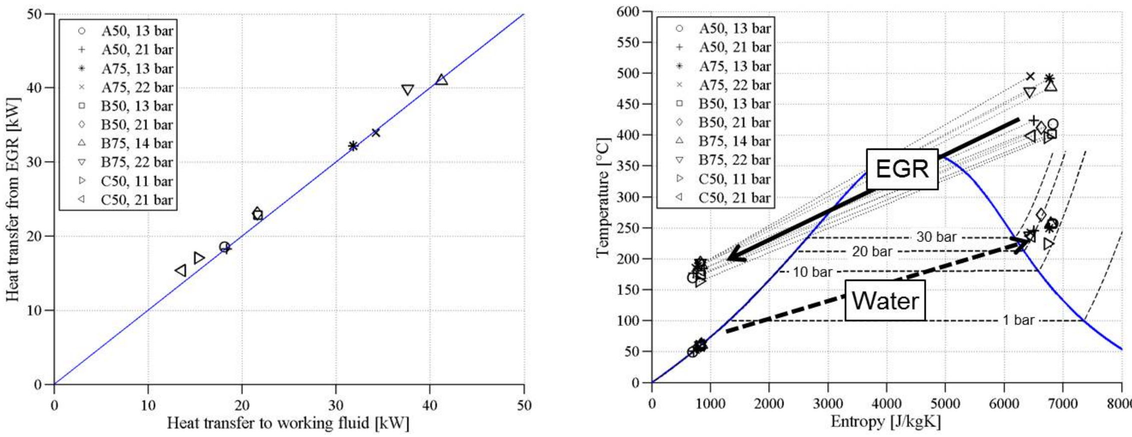

Figure 5: Heat transfer in the EGR boiler (left) and T-s diagram comparing fluid and EGR temperatures (right) at various ESC operating points and boiling pressures without an EGR after-cooler

To overcome the EGR temperature problem, an EGR after-cooler was designed that was intended to provide sufficient cooling and have minimal impact on the design of the EGR system (avoiding flow restrictions and any need for additional piping and brackets). The designed after-cooler replaced a horizontal section of the EGR route just before the EGR mixes with the charge air, and consists of a jacketed stainless steel pipe of identical diameter to the EGR pipe, supplemented with a helical copper coil inside. The jacket is cooled in parallel-flow configuration to the EGR, with the outlet water streaming through the copper coil in counter-flow direction to the EGR. This provides stable EGR temperatures below 80ºC at all considered operating points. The after-cooler mounted in the EGR route as well as the distribution of EGR heat between the boiler and after-cooler is shown in **Figure 6**. Up to a third of the EGR heat goes to the after-cooler. The impact of the boiling pressure on this fraction is rather weak and less systematic than expected. However, at operating points with lower EGR temperatures (e.g. B50 and C50), high boiling pressures cause a reduction of heat utilization in the boiler due to the pinch-point limitation.

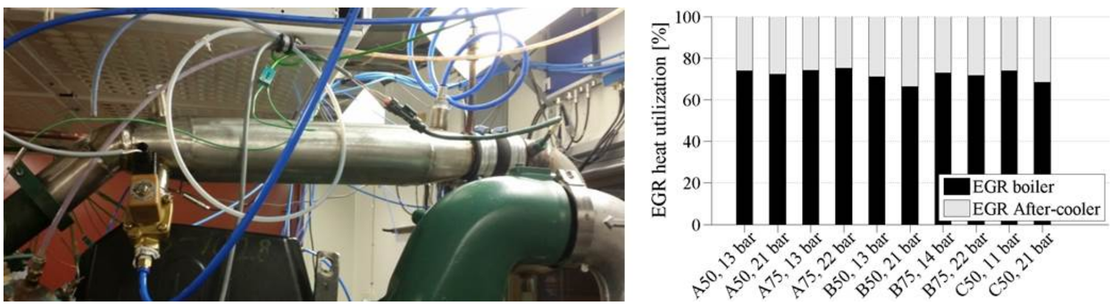

Figure 6: EGR after-cooler in the EGR route (left), distribution of EGR heat when cooled to 80ºC (right)

3.2 Experiments with expander engaged

Following the tests with the bypassed system, the operation and performance of the current expander design was evaluated. Engine oil with SAE classification 15W40 was used for these initial tests. The oil circuit of the expander is constructed as a dry sump system, in which the external oil tank was electrically heated to 120ºC to evaporate water from the lubrication system quickly and return the steam to the system downstream of the expander, as illustrated in **Figure 1**.

Figure 7 shows the steam boundary conditions and performance of the expander during a test in which the load was increased from B50 (with saturated vapor) to B65 (with superheated vapor) to assess responses of the heat recovery system's efficiency and expander power output to the associated increases in inputs. The steam pressure increased due to the heat input. The expander speed was 600 rpm during the test (further increases of speed had no positive effect on power output). To assess the thermal efficiency of the Rankine cycle, the power output is related to the heat transferred in the boiler, while the expander's efficiency is assessed in terms of the isentropic enthalpy drop of the fluid over the expander. A general conclusion from this test is that the thermal efficiency achieved (between 5 and 10 %) is rather poor compared to the highest values reported in similar studies, as summarized for instance by Sprouse and Depcik (2013). This is because the expander used for the tests does not perform well, in the current configuration, under the given boundary conditions. Increasing the inlet steam pressure from 20 to 30 bar helps to double both the expander and thermal efficiency, indicating that the optimum inlet pressure for the expander lies beyond these values. One way to address this issue would be to increase the inlet pressure for the expander beyond 30 bar, but this was regarded as inadvisable in such early stages of testing the EGR boiler prototype. Lowering the condensation-side pressure below atmospheric level was not attempted, due to the risk of problematic air infiltration into the system. The remaining option was to modify the expander design by extending the steam admission phase or lowering the geometrical compression-ratio. These concepts, which can be used for adapting a uni-flow expander to given limitations in inlet pressures, are discussed in section 3.3.

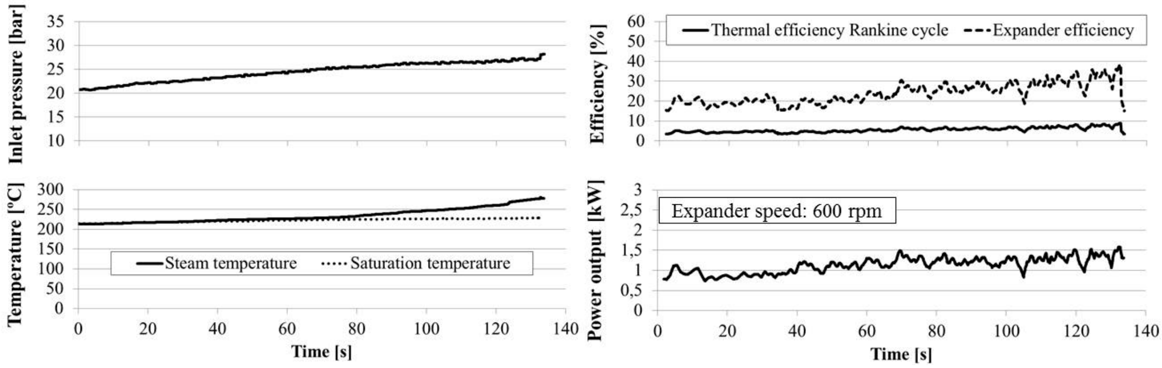

Figure 7: Boundary conditions (left) and performance (right) during an increase in load from B50 to "B65"

During expander operation, perceptible contamination of the working fluid with oil and vice versa was observed due to blow-by, resulting in unacceptable reductions in the oil's viscosity and hence the expander oil pressure for lubrication of the expander bearings. The water separation capability of the oil was poor and evaporation of the working fluid from the oil in the tank too inefficient to address these problems. Consequently, the oil was replaced with special steam engine oil, with a kinematic viscosity of 290 mm^2/s at 40°C (DIN 51562-1), which has better properties in the presence of water.

3.3 Expander simulations

Effects of varying several parameters were investigated using the GT-Suite piston expander model. A particular objective was to assess potential strategies to improve the performance of a uni-flow expander when admission pressure is limited. One possibility is to decrease the expander compression ratio, and hence re-compression pressure (thereby shifting down the pressure required for efficient expander operation). Another alternative is to extend the admission phase by closing the inlet valve later in the expansion stroke, thus allowing more steam to enter the cylinder. The results indicate that at constant pressure boundary conditions both strategies provide similar increases in power output, but also similar increases in steam consumption.

The modeled dependence of the expander power output, and associated steam consumption, on the steam inlet pressure, compression ratio and expander speed are mapped in **Figure 8**. For comparison, the steam flow rates the boiler can supply at stable superheating levels are also listed. Projecting the 20-30 bar inlet pressure (at 600 rpm) for the experimental operating point characterized in **Figure 7** on these maps, it can be seen that the power output between 1 and 2 kW can be confirmed by the expander model for the baseline compression ratio of 21. From the speed variation in the expander maps, it can be seen that increasing the expander speed beyond 600 rpm gives no improvement in power output at this compression ratio since the low inlet pressure is the power-limiting factor. The steam flow rate measured during the expander test described in section 3.2 could not exceed 6 g/s for this reason, which also caused the superheating temperature to increase over time (**Figure 7**). The model predicts a steam flow rate of 5 g/s for the same operating point. This deviation between the experimental and simulation results may be due to blow-by losses, which are not included in the simulation results.

It can also be seen that by reducing the compression ratio from 21 in the current design to 13, the expander could be operated at lower steam inlet pressure, achieving up to 3 kW in power output with 30 bar inlet pressure at a B50 operating point. In practice, this could be achieved by mounting a distance plate between the cylinder housing and crankcase of the expander, thus increasing the dead cylinder volume at piston top dead center. A consequence would be a 40% increase in steam consumption at this operating point, but the measured steam delivery rates of the boiler indicate that this could be covered. At the same configuration with a compression ratio of 13, an expander power output of 5 kW at 1200 rpm could be achieved for the B75 operating point. These results underline the sensitivity of the uni-flow piston expander's performance to the system pressures.

From the measured steam delivery rates of the boiler it can be seen that the flow rate of steam has very weak dependency on the two boiling pressure levels. While the pinch point limitation in the boiler lowers the utilizable EGR temperature difference at high boiling pressures, the heat of vaporization for water is up to 20% lower under these conditions (explaining why the flow rates can be maintained overall).

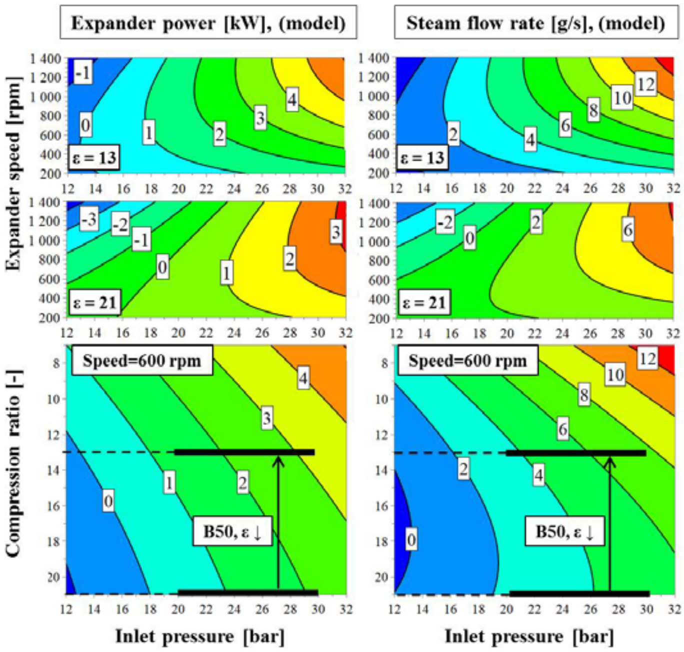

Delivery-rates of superheated steam from the EGR boiler (experiment)	
A50,13 bar	6.7 g/s
A50, 21 bar	6.9 g/s
A75, 13 bar	11.8 g/s
A75, 22 bar	12.9 g/s
B50, 13 bar	8.1 g/s
B50, 21 bar	8.1 g/s
B75, 14 bar	15.3 g/s
B75, 22 bar	14.4 g/s
C50, 11 bar	5.8 g/s
C50, 21 bar	5.2 g/s

Figure 8: Modeled expander power and steam flow rate as functions of expander speed, compression ratio ε and inlet pressure (left). List of measured steam-delivery rates of the EGR boiler prototype (right).

3.4 EGR boiler simulations

Comparison of the LEM simulation and experimental data (**Figure 9**) reveals that the simulation over-predicts superheat in most cases. There may be many reasons for this, e.g. two-phase phenomena (model limitations in handling gravity or fluid separation, for instance), inaccuracies of coefficients and correlations (related to fluids and geometry), other model limitations (e.g. channel-to-channel variations), fouling (which is ignored in the presented model), and heat losses to the surroundings.

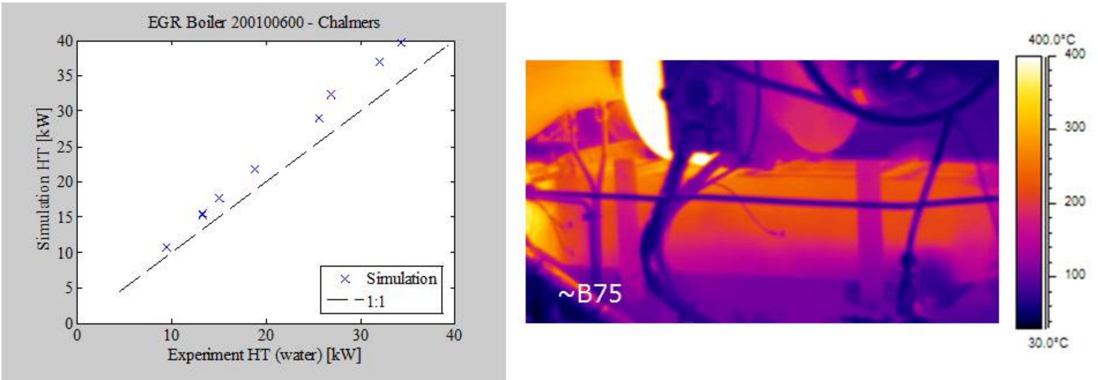

Figure 9: Comparison of simulation and experimental data (left). Engine load varies between A25 and B75, hence flows and pressures of both EGR and water also vary. Infrared image of the boiler side-plate (right). Fluid enters at the bottom right corner and exits at the top left corner. EGR flows from left to right.

Two-phase phenomena and characteristics in the EGR boiler were also explored in CFD simulations. Details are beyond the scope of this article, but the simulations revealed clear internal circulation on the fluid side: most of the liquid fluid immediately turns and flows along the bottom of the heat-exchanger. It gradually evaporates along the way and expands into the center region. However some of the vapor turns and flows in the reverse direction, creating a large steam “bubble” over the channel section that reduces both the effective heat transfer area and temperature difference, thereby reducing the overall heat-exchanger efficiency. This is likely the main reason for the difference between the LEM predictions and experimental data. It should be noted here that the engine, and hence boiler, are mounted in the same fashion in the test rig as in the truck, with a 4° angle to the horizontal plane, which further drives the liquid forward in the bottom of the vertical channels. Infrared images of the side-plate (**Figure 9**) support the CFD predictions, indicating that temperatures are significantly lower at the bottom of the heat-exchanger. The outer channel on the boiler is a fluid channel but the thick side-plate smears much of the gradients due to axial conduction in the wall. The images still clearly show that the liquid phase is not distributed over the height.

4. CONCLUSIONS

The goal of this study was to identify and characterize design component-level challenges associated with using a Rankine cycle-based system to recover waste heat from the EGR of a heavy-duty Diesel engine. The approach was to closely couple experiments using a full-scale demonstrator test bench system with simulations of processes in the EGR boiler and piston expander to highlight parameters and features that strongly influence the system’s overall performance. Water was used as the working fluid as it has promising potential in terms of both efficiency and convenience for applications at the considered heat-source temperatures.

The EGR boiler was designed as a plate-heat exchanger with vertical plates to investigate gravity effects in the boiler. CFD simulations and infrared images taken during the experiments showed the presence of internal flow circulation in the boiler. A steam “bubble” was formed, staying in the upper part of the boiler and reducing the area of effective heat transfer to the working fluid. The cooled EGR temperatures after the boiler were high (particularly at the A75 and B75 load points: up to 200ºC, which is more than twice the temperature in degrees Celsius than the engine’s standard EGR cooler provides). Thus, an EGR after-cooler that further cooled the EGR to 80ºC was built and mounted in the EGR route.

The maximal thermal efficiency of the system was just 10%, but the piston expander was not designed for use in the applied boundary conditions. A major bottleneck was the high re-compression of exhaust steam due to the uni-flow operational mode. A 1D simulation model for the expander indicated that either reducing the compression ratio or extending the steam admission phase could double the expander's power output at current steam-delivery rates from the EGR boiler.

NOMENCLATURE

CFD	Computational fluid dynamics
EGR	Exhaust gas recirculation
ESC	European Stationary Cycle
ε	Compression ratio
HT	Heat transfer
LEM	Lumped element model
OSF	Offset strip fin
ORC	Organic Rankine cycle
TDC	Top dead center
UDF	User-defined function

REFERENCES

Edwards, S., Eitel, J., Pantow, E., Geskes, P., Lutz, R., 2012, Waste Heat Recovery: The Next Challenge for Commercial Vehicle Thermomanagement, *SAE Int. J. Commer. Veh*, vol. 5, no. 1, p. 395-406.

Horst, T., Tegethoff, W., Eilts, P., Koehler, J., 2014, Prediction of dynamic Rankine Cycle waste heat recovery performance and fuel saving potential in passenger car applications considering interactions with vehicles' energy management, *Energy and Conversion Management*, vol. 78, p. 438-451.

Howell, T., Gibble, J., Tun, C., 2011, Development of an ORC system to improve HD truck fuel efficiency, *Deer Conference 2011*, Detroit, Michigan, USA.

Latz, G., Andersson, S., Munch, K., 2013, Selecting an Expansion Machine for Vehicle Waste-Heat Recovery Systems Based on the Rankine Cycle, *SAE Technical Paper* no. 2013-01-0552.

Lemmon, E.W., Huber, M.L., McLinden, M.O., 2013, *NIST Standard Reference Database 23: Reference Fluid Thermodynamic and Transport Properties-REFPROP*, Version 9.1, National Institute of Standards and Technology, Gaithersburg.

Panesar, A., Morgan, R., Miché, N., Heikal, M., 2013, Working fluid selection for a subcritical bottoming cycle applied to a high exhaust gas recirculation engine, *Energy*, vol. 60, p. 388-400.

Rayegan, R., Tao,Y.X., 2009, A critical review on single component working fluids for organic Rankine cycles, *ASME Early Career Technical Journal*, vol. 8, no. 2, p. 1-8.

Ringler, J., Seifert, M., Guyotot, V., Hübner, W., 2009, Rankine Cycle for Waste Heat Recovery of IC Engines, *SAE Technical Paper* no. 2009-01-0174,

Seher, D., Lengenfelder, T., Gerhardt, J., 2012, Waste Heat Recovery for Commercial Vehicles with a Rankine Process, *21st Aachen Colloquium Automobile and Engine Technology*.

Sprouse, C., Depcik, C., 2013, Review of organic Rankine cycles for internal combustion engine exhaust waste heat recovery, *Applied Thermal Engineering*, vol. 51, p. 711-722.

Stobart, R, Weerasinghe, R., 2006, Heat Recovery and Bottoming Cycles for SI and CI Engines – A Perspective, *SAE Technical Paper* no. 2006-01-0662.

Stumpf, J., 1912, *The una-flow steam engine*, R. Oldenbourg, Munich, 1912.

Struzyna, R., Eifler, W., Menne, A., 2014, Suitability of selected working fluids for use in Waste-Heat-Recovery units, *IAV 4th Thermoelectrics Conference*, Berlin.

Wagner, W., Pruss, A., 2002, The IAPWS Formulation 1995 for the Thermodynamic Properties of Ordinary Water Substance for General and Scientific Use, *J. Phys. Chem. Ref. Data*, vol. 31, no. 2, p. 387-535.

Wang, T., Zhang, Y., Peng, Z., Shu, G., 2011, A review of researches on thermal exhaust heat recovery with Rankine cycle, *Renewable and Sustainable Energy Reviews*, vol. 15, p. 2862-2871.

Webb, R.L., Kim, N.-H., 2005, *Principles of Enhanced Heat transfer*, 2nd edition, CRC Press, London.

ACKNOWLEDGEMENT

This study was conducted as a part of a waste-heat recovery project supported by the Swedish Energy Agency. The authors gratefully acknowledge the Agency's financial support.